Ashfold, M. N. R., Murdock, D., & Oliver, T. A. A. (2017). Molecular photofragmentation dynamics in the gas and condensed phases. *Annual Review of Physical Chemistry*, *68*, 63-82. https://doi.org/10.1146/annurev-physchem-052516-050756

Molecular Photofragmentation Dynamics in the Gas and Condensed Phases

Michael N.R. Ashfold, Daniel Murdock and Thomas A.A. Oliver

School of Chemistry, University of Bristol, Bristol, U.K., BS8 1TS

Abstract

Exciting a molecule with a UV photon often leads to bond fission, but the final outcome of the bond cleavage is typically both molecule and phase dependent. The photodissociation of an isolated gas-phase molecule can be viewed as closed system: energy and momentum are conserved, and the fragmentation is irreversible. The same is not true in a solution-phase photodissociation process. Solvent interactions may dissipate some of the photoexcitation energy prior to bond fission, and will dissipate any excess energy partitioned into the dissociation products. Products that have no analogue in the corresponding gas-phase study may arise by, for example, geminate recombination. Here we illustrate the extents to which dynamical insights from gas-phase studies can inform our understanding of the corresponding solution-phase photochemistry and how, in the specific case of photoinduced ring-opening reactions, solution-phase studies can in some cases reveal dynamical insights more clearly than the corresponding gas-phase study.

Keywords

photochemistry, photodissociation, photoinduced ring opening, non-adiabatic dynamics, conical intersections.

1. HISTORICAL CONTEXT

Ciamician is recognised as a pioneer of (organic) photochemistry and an early advocate for fuel production by means of artificial photo'synthesis'.[1] His studies were performed in solution and usually driven by sunlight, at a time when the concept of the photon was yet to be fully accepted. Identifying the ultimate reaction products was in itself a major achievement, and any ideas regarding reaction mechanism were rudimentary. Even the concatenation of ideas like ground and excited electronic states, radiative and non-radiative transitions, spin multiplicity, *etc*, into what would later be termed a Jablonski diagram [2] still lay far in the future.

A potentially more fruitful path at that time for those curious about the mechanisms of photochemical reactions was to focus on very simple molecular systems – diatomic and 'diatomic-like' molecules. Bodenstein noted the decomposition of HI on exposure to light in 1908 [3] and, by 1913, was using photolysis instead of heat to initiate the Cl_2/H_2 chain reaction.[4] Mechanistic understanding improved rapidly during the 1920's, with the arrival of quantum mechanics, the Schrödinger equation and the Born-Oppenheimer separation. These concepts had huge impact on this field – as can be seen by perusing the 1929 Faraday Discussion on 'Molecular Spectra and Molecular Structure' in Bristol,[5] or the 1931 Discussion on 'Photochemical Processes'.[6] More intense (though still incoherent and generally polychromatic) light sources were now available, and the development of grating spectrometers enabled the recording of electronic absorption spectra for many small gas-phase molecules. Vibrational and even rotational fine structure was resolved and interpreted in many such spectra, enabling characterisation of excited electronic states. Regions of continuous absorption were also recognised in the plate spectra of, for example, the methyl halides, and correctly attributed to prompt dissociation into fragments that, necessarily, were born with high kinetic energy.[7] In other cases, the sharpness of structure within a progression of bands in the electronic absorption spectrum of a polyatomic molecule (*e.g.* NO_2) was seen to evolve; well resolved fine structure observed at lower excitation energies became progressively more diffuse as the excitation energy was increased. This was attributed to a loss of rotational quantisation, and the term 'predissociation' was coined.[8] Mechanism and dynamics were entering photochemical thinking.

This heralded the start of a sub-discipline specifically addressing the dynamics of photoinduced molecular fragmentation processes. Terenin reported wavelength dispersed fluorescence from electronically excited OH and CN fragments formed by vacuum ultraviolet (UV) photolysis of molecules like H_2O and CH_3CN in the gas phase.[9] Spectral analysis gave clues about the partitioning of (ro)vibrational energy in the dissociation products, and inspired related studies by, for example, Okabe.[10] Technology continued to advance: flash photolysis was coupled with kinetic absorption spectroscopy, ushering in the study of photodissociations yielding non-fluorescent (*e.g.* ground state) fragments. [11-13]

Then came the laser, offering many new opportunities for photochemists. The monochromaticity of laser light allowed much better definition of the photolysis energy than when using a broadband flashlamp. Laser light is coherent, directional and could be produced in short duration pulses. Taken together, these properties translated into much higher light intensities in the interaction volume containing the gas-phase sample of interest. Pulsed lasers were thus very well suited to use with molecular beams, enabling experiments at sufficiently low pressures to allow use of time-of-flight (TOF) coupled with mass spectrometric detection methods.[14,15] Photofragment translational spectroscopy (PTS) had arrived. Proponents of the method were now able to determine not just the primary products of a photodissociation under 'collision-free' conditions (*i.e.* free of any potential ambiguities introduced by secondary collisions), but also their relative yields (*i.e.* branching ratios) and, from their recoil velocity distributions, the energy disposal within these various products. The recoil velocity distributions contain speed *and* angular information. Laser light is usually linearly polarised, and will thus selectively excite parent molecules that have their transition dipole moment $\boldsymbol{\mu}$ aligned parallel to the electric vector ($\boldsymbol{\varepsilon}$). Provided the photoexcited molecules dissociate promptly (*i.e.* before rotational motion degrades the photoinduced alignment), this alignment will reveal itself as an anisotropy in the fragment recoil velocity distribution.[16,17] Measuring this distribution can provide insights into the symmetry of the photoexcitation process and the rapidity (or otherwise) of the subsequent fragmentation.

With the advent of the dye laser, the experimentalist for the first time had potentially fine control over the choice of excitation wavelength – ushering in laser induced fluorescence [18,19] and then resonance enhanced multiphoton ionisation (REMPI) [20] detection methods. Both rely on the target species having a suitably long-lived excited state, so neither is universal to all photofragments. When applicable, however, these probe methods can be enormously powerful – enabling quantum (*i.e.* spin-orbit, vibrational, rotational, fine-structure) state-specific detection of small fragments, and the determination of recoil velocities, $\boldsymbol{v}$ (via Doppler broadening of the transition lineshape), and subtle vector correlations between $\boldsymbol{\varepsilon}_{\text{probe}}$ and $\boldsymbol{v}$, between $\boldsymbol{\varepsilon}_{\text{probe}}$ and the rotational angular momentum, $\boldsymbol{J}$, and even the mutual correlation between $\boldsymbol{v}$ and $\boldsymbol{J}$.[21-23]

The development of REMPI detection methods also enabled the emergence of ion imaging [24,25] and then velocity map imaging (VMI) [26] as successors to the traditional PTS experiment. Key to this advance was the fact that, rather than using a mass spectrometer to detect the neutral fragment of interest after TOF separation, the product could now be ionised selectively at its point of creation, and accelerated onto a time- and position-sensitive detector. In favourable cases (and we caution that most of the photofragments that have been probed in this way are atoms or diatomics), this affords an orders of magnitude increase in collection efficiency. The choice of probe wavelength determines the product quantum state under study, the TOF of the ionised particle to the detector defines (or

confirms) the product identity (its mass to charge ratio), and the radial and angular shape of the detected image reports on the product recoil velocity distribution.[27] Subsequent advances include the development of different slice-imaging strategies, which remove the need to reconstruct the full 3-D velocity distribution from the 2-D projection recorded on the detector.[28,29] Welge's group pioneered a variant of the method, wherein H (or D) photofragments of interest were again 'tagged' at the point of formation by exciting not to (or above) the ionisation limit, but to a Rydberg state with high *n* principal quantum number.[30] Relative to VMI, the H (Rydberg) atom PTS method displays much poorer collection efficiency, but constitutes the gold standard when it comes to velocity resolution and has advanced our understanding of the primary photochemistry of numerous hydride molecules.[31,32]

Advances in wavelength tunability were matched by advances in short pulse laser technology. Following the lead set by Zewail,[33] ultrafast pump-probe methods are now used to 'clock' the evolution of a photoexcited molecule to its neutral dissociation products [34] and, using time-resolved photoelectron spectroscopy methods, to explore the very early time motions of the molecule following photoexcitation.[35,36] In many ways, the last few decades have been a golden time for those exploring the intimate dynamics of gas-phase molecular photodissociation processes – not least because the spectacular practical advances summarised above have been matched by arguably even more impressive advances in the sophistication and accuracy of electronic structure theory and calculations, in methods for propagating the nuclear motions on the ground and excited state potential energy surfaces (PESs), and for treating the non-adiabatic couplings by which molecules transition between these PESs.[37-39]

Given the arsenal of experimental and computational capabilities now available, one might assume that the field has reached a point where one could realistically expect to be able to unravel the photofragmentation dynamics of almost any small/medium sized molecule that can be conveniently introduced into the gas phase. In the case of near-UV excitations, at least, this is certainly truer now than ever before – but many exciting challenges remain. Extension to radical species,[40,41] to ever larger molecular systems (both neutrals and charged species),[42] to lower temperatures (ultracold chemistry),[43] to even shorter timescales (attochemistry) [44,45] and to much higher excitation energies using, for example, emerging X-ray free electron laser systems,[46,47] are just a few of the areas where we can anticipate significant advances in the coming years.

Many of these technological advances heralded step changes for solution-phase photochemists also. Here we summarise just some of the key developments most relevant to photoinduced molecular fragmentation processes. The idea that solvent molecules would constrain the separation of the primary photofragments and encourage their recombination – the 'cage effect' – can be traced back to the 1934 Faraday Discussion on 'Free Radicals',[48] and the distinction between rapid in-cage (*i.e.* geminate) and slower diffusive (*i.e.* non-geminate) recombination was recognised via experiments

involving steady state illumination of I_2 at different wavelengths in solvents of varying viscosity.[49] Flash photolysis enabled measurement of the electronic spectra of many organic radicals, and investigation of how these varied with solvent and, in the case of aqueous solutions, with pH.[50] Coupling flash photolysis with kinetic absorption spectroscopy allowed characterisation of triplet excited states of numerous organic molecules, and transient absorption studies soon extended to singlet excited states also once a short pulsed laser could be used in place of a flash lamp.[51] Such studies provided a wealth of new kinetic data pertaining to excited state lifetimes, to intersystem crossing and internal conversion rates, on the rovibrational cooling of photoproducts and the solvent dependences of all of these various processes, but revealed little dynamical insight. Indeed, it would be surprising if they had. Relative to the gas phase, the solution environment is characterised by orders of magnitude higher densities and by extensive disorder. Solute-solvent interactions inevitably introduce deactivation pathways for excited molecules and for photofragments that are not available to their gas-phase counterparts, and out-of-equilibrium rotational or translational energy distributions in any primary photoproducts will typically be cooled by such interactions in a matter of picoseconds.

Again, the arrival of lasers capable of delivering short pulses commensurate with these relaxation timescales opened the way to dynamical studies of systems far from equilibrium. I_2, I_2^- and I_3^- were popular early targets for quantifying cage effects [52] for exploring the relaxation of the vibrationally excited recombination products [53,54] and for studying vibrational wavepackets on a predissociative potential energy surface in solution.[55,56]

Solvents are not rigid or purely mechanical entities that surround solute molecules, but the solute-solvent dynamic dipolar and electrostatic interactions can have major influences on the outcome and time scales of chemical reactions.[57] The field of solvation dynamics has played an important role in understanding how 'hot', nascent photoproducts dissipate their excess energy by coupling to the solvent bath, and the spectral density of the solvent is now recognised as a key factor in determining the frequency (and mode) dependent 'cooling' rates of out-of-equilibrium, (ro)vibrationally excited photoproducts. [58-61]

The generation of sub-ps mid-infrared pulses heralded a new era enabling selective detection (via their distinct vibrational frequencies) of nascent photoproducts from photodissociation of, for example, metal carbonyls of increasing size [62,63] and complexity.[64] More reliable and sophisticated laser technologies ushered in further advances: sub-20 fs broadband laser pulses,[65] and the widespread adoption of white light supercontinuum probes coupled to fast CCD camera technology and multiple element diode array detectors [66] enabled access to the earliest moments of a bond cleavage.[67] Ultrashort UV laser pulses were key to observing very rotationally excited CN fragments from the photodissociation of ICN, for example, and the finding that, contrary to predictions from statistical

mechanical models using linear response theory, the rotational excitation of the CN fragments persisted for up to 10 ps in water at room temperature.[68]

Multi-dimensional optical spectroscopies are currently at the forefront of techniques suited to studying solution phase reactions. Two-dimensional (2-D) spectroscopies in the electronic or vibrational domains are capable of separating the homogeneous and inhomogeneous linewidths,[69,70] and interrogating the inter- and intra-molecular couplings in molecules, aggregates and materials. In the context of this review, 2-D electronic spectroscopy has opened up new opportunities for studying photoisomerisation reaction dynamics with unprecedented detail.[71]

The remainder of this Review is devoted to comparing selected molecular photodissociation processes in the gas and condensed phases.[57,72,73] Two themes have been chosen, to illustrate (i) the extents to which dynamical insights from gas-phase (isolated molecule) studies can inform our understanding of the corresponding solution-phase photochemistry and (ii) how, in the specific case of photoinduced ring opening reactions, solution-phase studies can provide dynamical insights complementary to (and in some cases more clearly than) those revealed by the corresponding gas-phase study.

2. NEAR UV PHOTODISSOCIATION OF PHENOLS AND THIOPHENOLS IN THE GAS AND CONDENSED PHASE.

The process of interest here is the fission of the bond linking the heteroatom, X (O or S), and the H atom. Figure 1a shows cuts through the multi-dimensional PESs for the ground and first two excited singlet states of 4-methylthiophenol (4-MePhSH) as a function of the S–H bond length, R_{S-H}. The corresponding cuts for other (thio)phenol (PhXH) systems show the same key features, and much of the narrative that follows will be couched in terms of a generic PhXH system. The potential energy curves (PECs) shown by solid lines apply for planar geometries. In this high (C_S) symmetry limit, the PEC of the ground (S_0) state of PhXH correlates diabatically with electronically excited PhX($\tilde{A}$) products (plus an H atom). The X atom in the PhX radical supports three non-bonding electrons, distributed between an out-of-plane (*a*'') and an in-plane (*a*') *p*-orbital. Viewed in this simple three-electron picture, the ground ($\tilde{X}$) and first excited ($\tilde{A}$) states of the radical have respective configurations $(a')^2(a'')^1$ and $(a')^1(a'')^2$ and, as Figure 1a shows, the in-plane approach of an H atom to PhX($\tilde{X}$) results in a repulsive interaction. This is the long range part of the PEC of an excited state of PhXH formed by promoting an electron from an occupied lone pair (*n*) or bonding (π) molecular orbital to a σ^* orbital localised around the X–H bond. Such excited states (henceforth termed $\pi\sigma^*$ states) are now recognised as playing key roles in the near UV photoinduced fragmentation dynamics of many families of molecules.[32,74,75] Figure 1a shows two further important features. The S_0 and $\pi\sigma^*$

PECs intersect at extended $R_{X–H}$ in the planar limit, but this crossing becomes a region of conical intersection (CI-2 in Figure 1a) once out-of-plane motions are included. The adiabatic parent → product correlations along $R_{X–H}$ for non-planar geometries are shown by the dashed black lines. Figure 1a also shows that the first excited (S_1) singlet state of PhXH reached by vertical excitation in the Franck-Condon region is not the πσ* state, but the first ππ* state (solid red curve). The ππ* and πσ* PECs also exhibit a conical intersection at much smaller $R_{X–H}$, which we label CI-1 to allow distinction from CI-2.

Figure 1 also shows four data sets for systems with X = S that illustrate some of the similarities and the differences between gas- and solution-phase photochemistry. Figures 1b-1d display data for 4-MePhSH, while Figure 1e shows results from photolysis of 4-MePhSMe. The presence of a methyl (Me) group in the 4-position of all molecules has little effect on the photofragmentation of interest.[76] However, the breaking bond in the final example is an S–Me rather than S–H bond, which definitely does impact on the fragmentation dynamics. Figure 1b shows the total kinetic energy release (TKER) spectrum obtained by measuring the TOFs of H atoms formed by 267 nm photolysis of jet-cooled, gas-phase 4-MePhSH molecules. The 4-MePhS fragments are formed in both the $\tilde{X}$ and $\tilde{A}$ electronic states, in a limited number of vibrational levels. The sharpness of the peaks in the TKER spectrum shows that the radicals are formed with little rotational energy. The H atom recoil velocity distributions are anisotropic, and the anisotropy is $\boldsymbol{v}$-dependent.[76]

Such detailed data, recorded at many near UV photolysis wavelengths, enables a detailed description of the dissociation dynamics.[76,77] Focussing on just the longer excitation wavelengths, molecules can be promoted to the πσ* PES directly – by photon absorption – or indirectly – by photoexcitation to the ππ* state and then tunnelling through the small energy barrier associated with CI-1. Having reached the πσ* PES, these molecules evolve towards CI-2. Here the population bifurcates: a fraction follows the adiabatic path (upper dashed curve in Figure 1a) to $\tilde{A}$ state radical products, the rest undergoes non-adiabatic coupling at CI-2, accesses the ground state PES and can dissociate to $\tilde{X}$ state products. This accounts for the two sets of features evident at higher TKER in Figure 1b, but we also see a further (isotropic) yield of products with low TKER. These are assumed to arise from the decay of highly internally excited 4-MePhSH(S_0) molecules, over longer timescales and via pathways that sample much more of the ground state PES before releasing the detected H atom.

PTS studies of gas-phase phenol molecules [78-80] reveal similar dissociation dynamics, but the vertical energy separation between the πσ* and ππ* states in PhOH [79,81-84] is much larger than in PhSH.[76,85] Long wavelength excitation of PhOH thus populates exclusively the ππ* state which, again, can decay by tunnelling through a (much larger) barrier under CI-1, but on an orders of magnitude longer

(nanosecond) timescale,[86] and subsequent non-adiabatic coupling at CI-2 to yield H + PhO($\tilde{X}$) products in a limited number of vibrational levels.

Analogous TKER data for the Me + 4-MePhS products formed following photoexcitation of the $S_1(\pi\pi^*)$–S_0 origin band of 4-methylthioanisole in the gas phase have been obtained by VMI measurements of the Me(v=0) products.[87] As in the photolysis of bare thioanisole,[88,89] the partner 4-MePhS fragments are formed with an inverted electronic state population distribution (*i.e.* mainly in the excited $\tilde{A}$ state), on a nanosecond timescale.[89,90] These observations accord with expectations that the PECs along $R_{S–Me}$ are qualitatively similar to those shown in Figure 1a. Fragmentation starts with an initial, rate limiting, coupling to the $\pi\sigma^*$ PES via CI-1. The requirements for tunnelling are much more stringent in the case of a heavier leaving group like CH_3, and the available data suggest that this non-adiabatic tunnelling probability is higher at non-planar geometries which are maintained as $R_{S–Me}$ extends further – thereby favouring the *adiabatic* dissociation path past CI-2, forming 4-MePhS($\tilde{A}$) products.[87] Exciting thioanisole on a few select parent absorption resonances in a narrow energy range above the S_1–S_0 origin results in very different $\tilde{A}/\tilde{X}$ state product ratios.[88,91] These 'dynamic resonances' are pictured as transitions to bound states embedded in the continuum generated by the conical intersection; their identification may provide insights into the nuclear motions that facilitate non-adiabatic coupling at CI-1 and/or CI-2.[92] Not surprisingly, phenol, thiophenol and thioanisole are attracting much interest as test-systems for honing the treatment of non-adiabatic effects in molecular photodissociations. [83,93-95]

The remaining panels in Figure 1 show data obtained following 267 nm excitation of these same systems in solution. Figure 1c shows broadband transient electronic absorption (TA) data for 4-MePhSH in cyclohexane, recorded at different pump-probe delays, *t*. The displayed spectra are the difference in absorption recorded at a given *t* with and without the prior UV pump pulse. A positive (*i.e.* absorption) feature centred at ~480 nm attributable to ground state 4-MePhS radicals [96,97] is evident within the ~100 fs instrument response time – consistent with ballistic S–H bond fission, as in the gas-phase photodissociation at similar wavelengths.[76] The profile of this feature sharpens with increasing *t*, and its amplitude has declined by ~30% at *t* = 200 ps. This narrowing reflects the dissipation of vibrational energy from the nascent 'hot' 4-MePhS($\tilde{X}$) radicals to the solvent bath, while the decline in amplitude is a signature of geminate recombination – thereby illustrating two of the additional dynamical complexities associated with solution phase photodissociation reactions.

The gas-phase studies show that ~40% of the 4-MePhS radicals from the 267 nm photolysis of 4-MePhSH are formed in their excited ($\tilde{A}$) state.[76] Ultrafast TA studies of the same photolysis in cyclohexane identified an absorption attributable to 4-MePhS($\tilde{A}$) products at very short pump-probe delay times. Extracting the *initial* product branching in a solution phase dissociation is challenging on

account of competing dynamical processes like in-cage recombination, which will encourage any incipient 4-MePhS($\tilde{A}$) + H products to re-sample CI-2 and either follow the diabat to reform S_0 parent molecules or re-cross the CI to yield 4-MePhS($\tilde{X}$) + H radicals. In this specific case, kinetic analyses and decay associated spectra suggest a strong preference for initial bond extension to 4-MePhS($\tilde{A}$) + H products [98] – in clear contrast to gas-phase studies at the same wavelength.[76,99] The initial $\tilde{X}/\tilde{A}$ product branching ratio estimated from equivalent studies of this same photolysis in ethanol is only ~0.8 – highlighting the different early-time dynamics prevailing in the different solution environments. Nonetheless, in both solvents, all 4-MePhS radicals are quenched to the $\tilde{X}$ state by t > 300 fs.[98]

As Figure 1c shows, another feature, centred at ~380 nm, becomes evident at later times (t > 5 ps) and grows with a time constant that matches the (partial) decay of the 4-MePhS($\tilde{X}$) radical signal. This 380 nm band is the signature of an adduct formed by geminate recombination of the primary dissociation products, identified as the sulfur analogue of 2,4- (or 2,5-) cyclohexadienone (*i.e.* structures formed by the primary H atom photoproduct recombining with the ring). The fact that the amplitude of the ~480 nm feature does not decay to zero by t = 200 ps shows that some 4-MePhS($\tilde{X}$) radicals escape the primary solvation cage and remain separated from the geminate H atom partner. But the fact that it decays at all, and the assignment of the ~380 nm feature, both imply some recombination of the primary dissociation products. Geminate recombination surely results in reformation of the 4-MePhSH parent also, but TA data like that shown in Figure 1c is blind to this process, as the available white light supercontinuum probe does not extend to sufficiently short wavelengths to interrogate the electronic absorption of the ground state parent molecule.

Fortunately, time resolved infrared (TRIR) absorption spectroscopy can circumvent this limitation, as illustrated in Figure 1d for the case of 267 nm photolysis of 4-MePhSH in CD_3CN. Two features are clearly evident in these spectra at the earliest pump-probe delays: a negative-going parent bleach signal at ~1495 cm^{-1} and an absorption at ~1560 cm^{-1} attributable to 4-MePhS($\tilde{X}$) radical products. An additional weak feature at ~1630 cm^{-1} – attributable to the same adduct as that responsible for the ~380 nm absorption in the TA spectrum – grows in at later times.[100] The ~1560 cm^{-1} feature narrows and its centre shifts to higher wavenumber with increasing t – consistent with formation of vibrationally excited radicals that subsequently cool via interaction with the solvent. The radical signal peaks within the 1 ps response time of the TRIR experiment, and the kinetics of its decay match that determined by monitoring the parent bleach recovery. Analysis shows that ~40% of the total radical population undergoes geminate recombination within t = 150 ps and that 4-MePhSH(S_0) molecules are the dominant product from this recombination.[73,100]

The corresponding TRIR spectra taken following 267 nm photolysis of 4-MePhSMe (in CD_3CN, Figure 1e) also show three features: a bleach at ~1495 cm^{-1} that is partially overlapped by an intense transient absorption at ~1485 cm^{-1} – both of which are clearly present at the earliest delay times – and a weaker absorption at ~1570 cm^{-1} that grows with increasing *t*. As with 4-MePhSH, the bleach is attributable to photo-induced depopulation of the parent ground state, and the weak ~1570 cm^{-1} feature confirms 4-MePhS($\tilde{X}$) radical formation (by S–Me bond fission in this case). The more intense absorption at ~1485 cm^{-1} is a signature of electronically excited 4-MePhSMe(S_1) molecules. This excited state absorption (ESA) blue-shifts at early *t* (consistent with initial formation of internally excited 4-MePhSMe(S_1) molecules that relax to low vibrational levels of the S_1 state within a few picoseconds) and thereafter decays to zero by t = 1.5 ns. Kinetic analysis in this case returns solvent dependent rate coefficients, but the principal finding is that the dissociation rate constant (k_{diss}) scales with the amount of internal (vibrational) excitation: k_{diss} for the initially prepared 4-MePhSMe(S_1) molecules is several orders of magnitude larger than that for vibrationally relaxed 4-MePhSH(S_1) molecules.[100] Both findings mirror trends in excited state lifetime found in gas-phase studies of thiophenols and thioanisoles, and can be understood in light of the potential barrier associated with CI-1 (Figure 1a).

The above examples mostly involve relatively weakly interacting solvents like cyclohexane and acetonitrile, though we noted the stronger solute-solvent interactions when 4-MePhSH is dissolved in a more polar solvent (ethanol),[98] and that the detailed decay kinetics of 4-MePhSMe(S_1) are solvent dependent.[73] To emphasize the potential importance of solvent choice, Figures 2a and 2b compare TA spectra recorded following 267 nm photolysis of phenol (PhOH) in, respectively, cyclohexane and water. The early time traces in the former are dominated by a broad feature that spans the entire probe wavelength window and decays with a ~2.1 ns time constant. This is attributable to ESA by PhOH(S_1) molecules – an assignment supported by electronic structure calculations, time-correlated single photon counting measurements [98] and complementary TRIR data.[73] A structured feature at ~400 nm becomes increasingly obvious at later times. This signature of PhO($\tilde{X}$) radicals [101-103] develops on the same, nanosecond, timescale. These data all support the view that the mechanism for O–H bond fission following excitation to the S_1 state of PhOH in a weakly interacting solvent like cyclohexane is very similar to that operating in the gas phase, *i.e*. non-adiabatic tunneling through the substantial potential barrier under CI-1, followed by non-adiabatic coupling to the ground state PES at CI-2 and eventual formation of H + PhO($\tilde{X}$) products.

Figure 2b shows TA data recorded following 267 nm photoexcitation of phenol in water, a strongly interacting solvent with very interesting dynamical properties. Spectra recorded at early times (t < 1 ns) are again dominated by a (decaying) ESA attributable to the PhOH(S_1) state, supplemented by a (growing) feature at ~600 nm assigned to ESA of phenol excimers,[98,104] but show no signature

attributable to solvated electrons ($e^-_{(aq)}$). Appreciable yields of phenoxyl radicals and solvated electrons (the latter confirmed by electron scavenging experiments) are evident in TA spectra recorded at later times (t >2 ns) however, with a PhO($\tilde{X}$) radical yield of ~13% estimated at t = 13 ns. TA studies of the 267 nm photoexcitation of phenol-d_1 in D_2O return the same spectral features and very similar kinetics. In both cases, the ratio of PhO($\tilde{X}$) radicals to solvated electrons at late time delay (t = 14 ns) was determined to be ~1:1, implying negligible kinetic isotope effect. Such observations are incompatible with the tunneling mechanism advanced to explain O–H bond fission in the gas phase or in cyclohexane but could be explained by near-threshold autoionization from the PhOH(S_1) origin to the $PhOH^+_{(aq)} + e^-_{(aq)}$ asymptote followed by rapid deprotonation [105] or, possibly, in terms of an excited state proton-coupled electron transfer process.[106,107]

Summarising, there is a growing body of evidence to support the thesis that the fragmentation dynamics established from careful gas-phase studies can provide valuable insights into the early stages of the photodissociation of that same solute in a *weakly* interacting solvent. This is tantamount to saying that, in such cases, the underlying PESs and the non-adiabatic couplings that govern the dissociation of the isolated molecule are not substantially perturbed when the molecule is in the presence of a weakly interacting solvent. Recent studies of BrCN photolysis in perfluorohexane – an essentially non-interacting solvent – represent an extreme exemplar of this statement.[108] But the foregoing examples also highlight the need for care when making such extrapolations. The dissociation of an isolated gas-phase molecule constitutes a closed problem; energy, linear and angular momentum are conserved. Viewed from the perspective of a dissociating molecule, the equivalent problem in the condensed phase is non-conservative. Solvent interactions may redistribute part of the photoexcitation energy within the solute molecule and some of this energy may dissipate to the solvent, prior to bond fission. Any excess energy in the fragmentation products formed upon bond fission will also rapidly transfer to the solvent bath, and 'products' that have no analogue in the corresponding gas-phase study may arise as a result of, for example, vibrational relaxation leading to trapping in particular product wells and/or geminate recombination. Assuming the applicability of insights from gas-phase studies to the photodissociation of a molecule in a *strongly* interacting solvent is more dangerous, however – as illustrated by the foregoing comparison of the 267 nm photolysis of phenol in the gas phase, in cyclohexane and in water, and by recent studies that contrast aspects of the near UV photochemistry of adenine in water with the findings from many previous gas-phase studies.[109]

3. PHOTOINDUCED RING OPENING: HOW SOLUTION-PHASE PHOTOFRAGMENTATION STUDIES CAN PROVIDE INSIGHTS INTO ISOLATED MOLECULE DYNAMICS.

The primary outcome of photoexcitation in the foregoing examples is bond fission, resulting in the formation of two fragments. Most reported photofragmentation dynamics studies involve such systems. But we recognise another family of photoinduced bond fissions, wherein a cyclic molecule transforms into a ring-opened isomer. Dynamical studies of such processes are much rarer, unsurprisingly, given (i) this community's traditional preference for gas-phase (isolated molecule) conditions, (ii) the large accompanying geometry change, which is likely to ensure that the ring-opened products are formed with high levels of internal (vibrational) excitation, and (iii) the fact that, without subsequent collisional relaxation, measurement and assignment of spectra of ring-opened species are likely to be challenging. Indeed, the internal energy within the nascent ring-opened isomer may well be sufficient to allow further isomerisation, and even dissociation. For example, Blank *et al*.[110] suggested a sequence of internal conversion, ring-opening, subsequent H-atom migration and molecular elimination on the ground state PES as a route to forming the HCN products observed in PTS studies of the 193 nm photolysis of pyrrole.

We now extend the simple few-electron picture used to rationalise CI-2 and the electronic branching in the radicals formed following S–H bond fission in PhSH to show how photoinduced asymmetric ring-expansion in heterocyclic molecules can actually drive non-adiabatic population transfer (*i.e*. internal conversion) to the S_0 PES and potentially result in ring opening. Figure 3a shows the occupancy of key orbitals in the ground and πσ* excited states of PhSH, and in the H + PhS($\tilde{X}$ / $\tilde{A}$) products. The molecule is constrained to be planar and the important occupied orbitals in the PhSH(S_0) state are taken as the non-bonding sulfur $p_x(a'')$ orbital and the $\sigma_{S-H}(a')$ orbital localised on the breaking bond. In this representation, the ground state parent has configuration $(a')^2(a'')^2$, the dissociative πσ* state is described as $(a')^2(a'')^1(\sigma_{S-H}^*, a')^1$, the $\tilde{X}$ and $\tilde{A}$ states of the PhS radical have respective configurations $(a')^2(a'')^1$ and $(a')^1(a'')^2$, and the parent→product correlations are as shown by the solid black lines in Figure 1a. Figure 3b shows the analogous picture for (planar) thiophene, with the important σ and σ* orbitals now centred on an S–C bond. Rupturing this bond results in a biradical with *a*'' symmetry (if occurring on the diabatic πσ* PES) or *a*' symmetry (on the diabatic S_0 PES). In this limit, therefore, we should anticipate a conical intersection between these PESs at extended R_{S-C} bond lengths. Henceforth, we will again label this as CI-2, since the long wavelength UV absorption of thiophene involves π*←π excitation, but the resulting ^{1}ππ* state population can access the πσ* state via a conical intersection between the ^{1}ππ* and ^{1}πσ* PESs (CI-1) at much shorter R_{S-C} bond length.[111-116] Imposing planarity and neglecting further (*e.g*. H-migration) isomerisations that could stabilise the primary biradical hampers direct comparison with experiment, but Figure 3 suffices to show that πσ*-state mediated ring-expansion could offer a route for non-adiabatic population transfer to the S_0 PES and subsequent ring-opening. Indeed, such photo-induced ring-openings have now been explored theoretically in several heterocyclic systems, including

furan,[117-119] pyrrole,[120] imidazole,[121] 2-aminooxazole,[122] adenine,[123] spiropyran, [124,125] and β-glucose.[126] Here we focus on experimental studies, however, illustrating how condensed-phase experiments can actually outdo gas-phase studies when seeking definitive evidence for, and mechanistic insight into, photoinduced ring-opening reactions.

Ultrafast pump-probe photoelectron spectroscopy (*i.e.* gas-phase) studies of thiophene reveal a very fast excited state decay, but the attribution of this decay to ring-opening relies on supporting theory.[112] Identifying a measurable that unarguably reveals the initial dynamics is a key challenge for experimental investigations of photoinduced ring-opening. Hence the appeal of substituted heterocycles bearing a 'reporter' group, whose spectral signature changes as the system evolves from the ring-closed to a ring-opened isomer. Photoinduced ring opening in thiophenone (thiophene with one C–H group adjacent to the sulfur replaced by a C=O group), for example, is very well-suited to study by TRIR absorption spectroscopy. As Figures 4a and 4b show, 267 nm photoexcitation of thiophenone dissolved in acetonitrile leads to an immediate parent bleach signal at ~1685 cm^{-1} and a broad transient absorption centred at ~2150 cm^{-1}; the 'reporter', the carbonyl vibration in thiophenone evolves into a ketene stretch mode upon ring-opening.[127,128] The breadth of the ketene feature, and its subsequent narrowing and blue shift, show that the ring-opened product is formed highly vibrationally excited and then relaxes (within picoseconds) through coupling with the solvent bath. The amplitude of the parent bleach signal decreases with increasing pump-probe delays. Analysis shows that ~60% of the photoexcited molecules ultimately ring-close, reforming thiophenone. Similar 225 nm pump, TRIR-probe studies of furanone (the O containing analogue of thiophenone) in acetonitrile reveal many parallels – prompt ring-opening and subsequent cooling of the vibrationally excited ketene – but also a much lower (only ~10%) probability of parent reformation. Electronic structure calculations support the general picture outlined in Figure 3b, whereby initial $\pi^* \leftarrow \pi$ excitation (where the starting orbital is dominated by the heteroatom p_x orbital) and subsequent non-adiabatic coupling to the $\pi\sigma^*$ PES via CI-1 directs population towards CI-2, non-adiabatic transfer to the S_0 PES and eventual branching to, either, reform the ring-closed parent or form one, or more, ring-opened ketene products.[128]

Near UV photoexcitation of α-pyrone (2*H*-pyran-2-one) results in broadly similar isomerisation dynamics. TRIR spectra measured at short *t* reveal prompt formation of (at least) two ring-opened ketene isomers with an *E*-configuration with respect to the central C=C double bond and ~68% probability for reforming the ring-closed starting molecule by t = 100 ps.[129] Measurements at longer pump-probe delay times (out to 100 μs) identify two further (thermally driven) isomerisations attributable to, first, thermalisation of the initially produced *E*-isomer population and, second, *E*- $\rightarrow$ *Z*-isomerisation (involving net rotation about the C=C double bond) resulting in almost total eventual recovery of the ring-closed parent population.[130,131] The early time nuclear dynamics involve $\pi\sigma^*$-

state mediated, asymmetric ring-expansion towards regions of conical intersection with the S_0 PES characterised by one much extended $R_{C–O}$ bond length and a non-zero torsional angle between the carbonyl and ketene moieties.[129] Electronic structure calculations for coumarin (benzopyron-2-one) identify what, structurally, appears to be a very similar conical intersection between the $\pi\sigma^*$ and S_0 PESs upon extending one C–O bond,[132] yet TA and TRIR absorption studies following UV excitation in this case reveal essentially 100% parent bleach recovery within 100 ps and no ring-opened products [129,133] – reminding us that the product branching is likely to depend not just on the geometry of, but also the nuclear momenta on passage through, the regions of conical intersection between PESs.

These examples illustrate how condensed-phase studies, together with appropriate theory, can provide dynamical insights into ring-opening processes that defy rigorous investigation by traditional gas-phase methods. But, having established the viability of such processes, we now highlight two recent gas-phase studies that also provide strong (albeit indirect) evidence for near UV photoinduced ring-opening in substituted thiophenes that, again, carry a suitable 'reporter' group. The first involves 2-iodo- and 2-bromothiophene, the photolyses of which have been probed via VMI measurements of the ground and spin-orbit excited halogen atom fragments.[134,135] The velocity distributions determined from images measured at longer UV wavelengths (*e.g.* 260–270 nm in the case of 2-bromothiophene) are consistent with prompt dissociation to Br + thienyl fragments on a repulsive PES populated via a parallel (to the breaking C–Br bond) transition. The images are reminiscent of those obtained when photolysing, for example, methyl bromide in its A-band.[136] As Figure 4c highlights, the Br/Br* images measured at shorter photolysis wavelengths (*e.g.* ~245 nm) are very different: notwithstanding the increase in photon energy, the images are smaller, and isotropic. Electronic structure calculations attribute this change in fragmentation behaviour to the opening of a rival C–S bond extension pathway leading to a conical intersection with the S_0 PES. The resulting ground state molecules are formed with sufficient internal energy to sample the configuration space associated with several parent isomers and dissociate to yield Br/Br* atoms in concert with both cyclic and non-cyclic partner fragments.[135] In similar vein, long wavelength ($278 \geq \lambda \geq 225$ nm) photolysis of 2-thiophenethiol results in cleavage of the pendant S–H bond and formation of H + thiophenethiyl products.[137] The deduced dissociation dynamics show many parallels with those for thiophenol and thioanisole (section 2). Most of the radical products are formed in their excited ($\tilde{A}$) state, consistent with a non-planar parent geometry on approach to CI-2. The TKER distribution changes upon tuning to yet shorter wavelengths, however, in a way that can be explained by again invoking the onset of a rival C–S bond extension pathway that enables non-adiabatic coupling via a conical intersection with the S_0 PES and subsequent unimolecular decay to, in this case, mainly H + thiophenethiyl($\tilde{X}$) products.[137] One key message emerging from the small but growing literature pertaining to photoinduced dynamics in heterocyclic systems is the importance of ring-based $\pi\sigma^*$ excited states in facilitating non-adiabatic coupling to the ground state: it is clear that incipient ring-expanding distortions can act as a driver for

radiationless transfer, even in situations that do not result in the formation of fully ring-opened products.

4. CONCLUSIONS

Any review of a field as extensive as that spanned by the present title will necessarily be selective. After a short historical introduction, we have focussed on comparing and contrasting the gas- and solution-phase photofragmentation dynamics of just two families of molecules: phenols and thiophenols and S or O containing heterocycles. Both highlight the pivotal role of $\pi\sigma^*$ excited states when describing the photoinduced bond cleavage. The former systems also serve to illustrate (i) the extent to which dynamical insights from high-resolution gas-phase studies can inform our understanding of the early time fragmentation dynamics in weakly interacting solvents, (ii) additional processes (*e.g.* vibrational energy transfer, geminate recombination, adduct formation, *etc*) that can contribute to the overall photochemistry displayed by these molecules in such weakly interacting solvents, and (iii) the dangers of assuming that dynamical insights from gas-phase studies of a given molecule extrapolate when the same solute is immersed in a strongly interacting polar solvent like water. The second examples illustrates how solvent interactions and rapid dissipation of internal energy within the primary photoproducts can be turned to advantage, enabling identification of dissociation pathways the operation of which would be hard to demonstrate, unambiguously, in the corresponding gas-phase study. Our selections emphasise the 'dynamics'-focus in the article title, but we recognise that other authors could easily have picked different systems to illustrate the potential symbiosis between gas- and condensed-phase studies – *e.g.* by focussing on progressively larger, involatile, thermally fragile, (bio)molecular solutes where solubility would progressively supplant volatility as the key requirement for any detailed experimental study.

DISCLOSURE STATEMENT

The authors are not aware of any affiliations, memberships, funding, or financial holdings that might be perceived as affecting the objectivity of this review.

ACKNOWLEDGEMENTS

Financial support from the Engineering and Physical Sciences Research Council (EPSRC; Programme Grant EP/L005913/1), the European Research Council (ERC, advanced grant 290966 CAPRI, to Professor A.J. Orr-Ewing) and the Royal Society (University Research Fellowship UF140231, to Dr T.A.A. Oliver) is acknowledged. The authors are also very grateful for many valuable discussions

with: Bristol colleagues, B. Marchetti, P.M. Coulter, R.N. Dixon, M.P. Grubb, S.J. Harris, R.A. Ingle, T.N.V. Karsili, H.J.B. Marroux, A.J. Orr-Ewing, G.M. Roberts and C.M. Western; I.P. Clark, G.M. Greetham, I.V. Sazanovich and M. Towrie at the Central Laser Facility at the Research Complex at Harwell; V.G. Stavros and his group (University of Warwick); and S.E. Bradforth and colleagues (University of Southern California).

Figure Captions.

Figure 1

(a) Potential energy curves for the S_0 and first excited $^1\pi\sigma^*$ (in black) and $^1\pi\pi^*$ (in red) states of 4-MePhSH, plotted as a function of $R_{S–H}$, illustrating CI-1 and CI-2; (b) TKER spectrum of the H + 4-MePhS products following 267 nm photolysis of gas-phase 4-MePhSH; (c) TA spectra measured at the displayed pump-probe delays following 267 nm photolysis of 4-MePhSH in cyclohexane; (d) and (e) TRIR absorption spectra measured at different pump-probe time delays over the wavenumber range 1400-1650 cm^{-1} following 267 nm photolysis of, respectively, 4-MePhSH and 4-MePhSMe in acetonitrile-d_3.

Figure 2

TA spectra measured over the wavelength range 350-650 nm at the displayed pump-probe delays following 267 nm photolysis of PhOH in (a) cyclohexane and (b) water solution. The inset in (b) shows the 380-500 nm region of the latter spectrum on an expanded vertical scale.

Figure 3

Schematic diagram highlighting parallels in the evolving occupancy of three key orbitals (the S($3p_x$) orbital (blue) and the σ (pink) and σ^* (green) orbitals localised around the extending bond) following photoexcitation leading to (a) S–H bond fission in PhSH and (b) C–S bond extension (ring-opening) in thiophene.

Figure 4

TRIR absorption spectra measured at different pump-probe time delays over the wavenumber ranges (a) 1550-1750 cm^{-1} and (b) 2000-2250 cm^{-1} following 267 nm photolysis of thiophenone in acetonitrile solution. Panel (c) shows images of ground state Br atoms formed by photolysis of gas-phase 2-bromothiophene molecules at 266.6 nm and at 244.9 nm, with the $\boldsymbol{\varepsilon}$-vector of the photolysis radiation aligned vertically as shown. The radius in these images, which were recorded under identical extraction conditions, is proportional to the Br fragment recoil velocity.

Figure 1

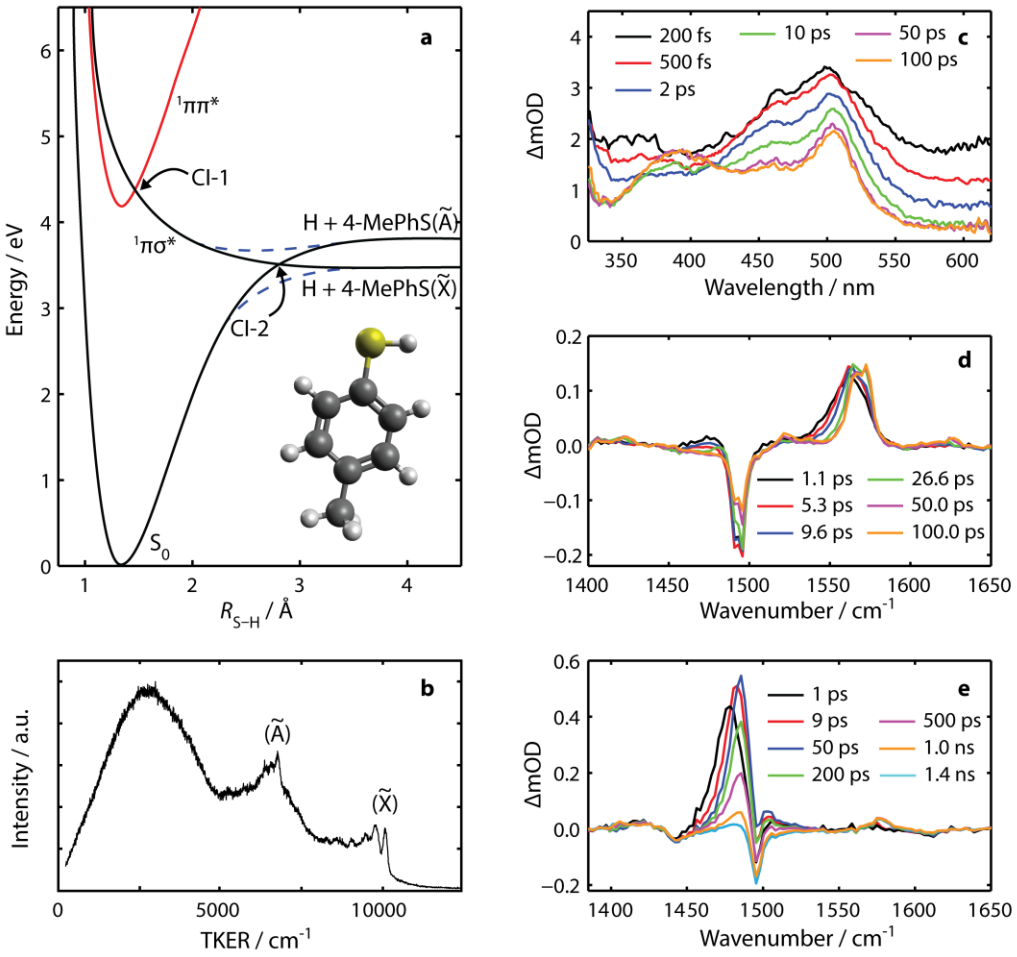
a
Energy / eV
R_{S-H} / Å
$^1\pi\pi^*$
CI-1
$^1\pi\sigma^*$
H + 4-MePhS(Ã)
H + 4-MePhS(X̃)
CI-2
S_0
b
Intensity / a.u.
TKER / cm^{-1}
(Ã)
(X̃)
c
ΔmOD
Wavelength / nm
200 fs
500 fs
2 ps
10 ps
50 ps
100 ps
d
ΔmOD
Wavenumber / cm^{-1}
1.1 ps
5.3 ps
9.6 ps
26.6 ps
50.0 ps
100.0 ps
e
ΔmOD
Wavenumber / cm^{-1}
1 ps
9 ps
50 ps
200 ps
500 ps
1.0 ns
1.4 ns

Figure 2

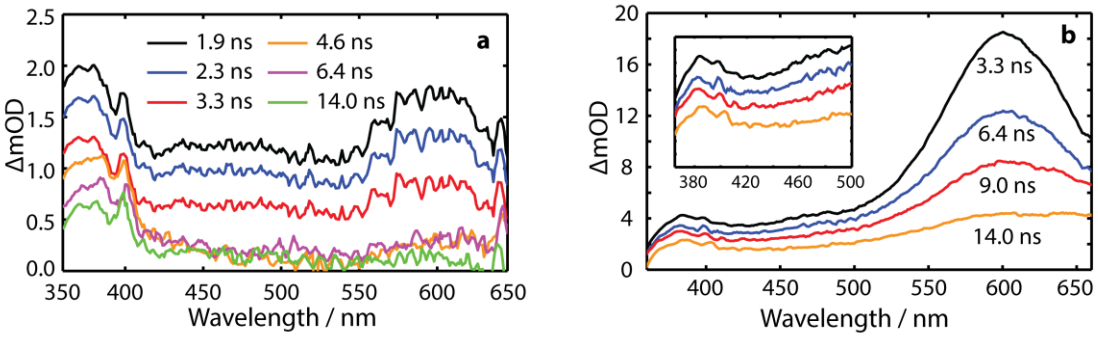
a
1.9 ns
2.3 ns
3.3 ns
4.6 ns
6.4 ns
14.0 ns
ΔmOD
Wavelength / nm
b
3.3 ns
6.4 ns
9.0 ns
14.0 ns
ΔmOD
Wavelength / nm

Figure 3

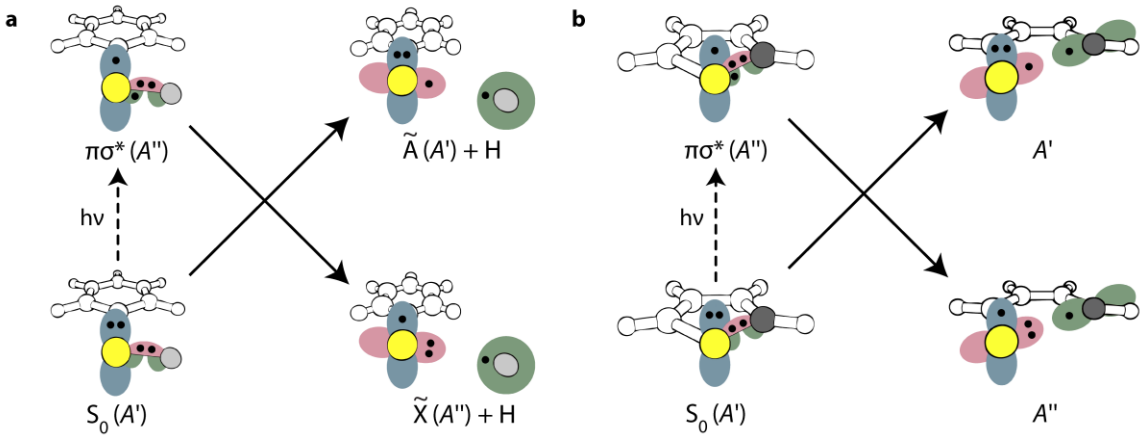

Figure 4

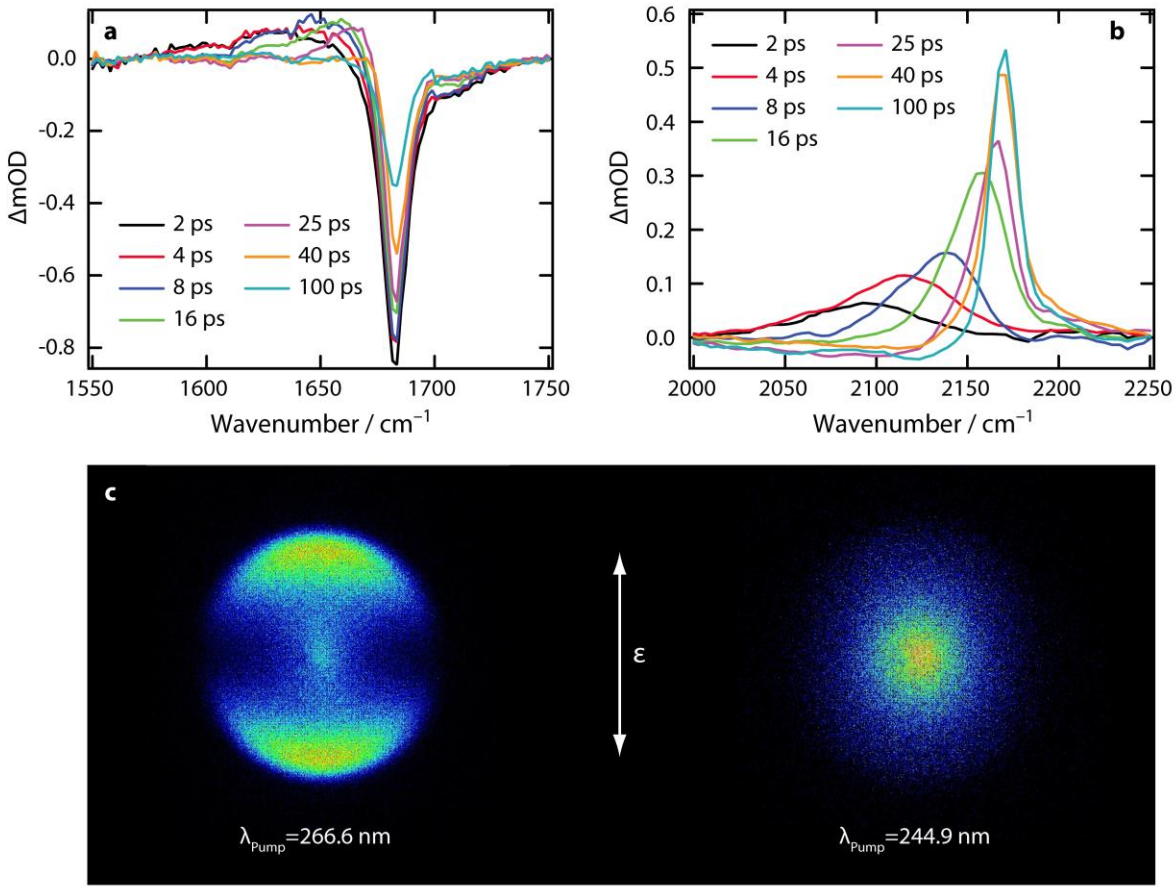
a
ΔmOD
Wavenumber / cm^{-1}
2 ps
4 ps
8 ps
16 ps
25 ps
40 ps
100 ps
b
c
ε
λ_{Pump}=266.6 nm
λ_{Pump}=244.9 nm

References

[1] Ciamician G. 1912. The photochemistry of the future. *Science* 36: 385-394.

[2] Jablonski A. 1933. Efficiency of anti-Stokes fluorescence in dyes. *Nature* 131: 839-840.

[3] Bodenstein M. 1908. Notice on decomposition of iodine hydrogen in light. *Z. Phys. Chemie* 61: 447-448.

[4] Bodenstein M, Dux W. 1913. Photochemische kinetik des chlorknallgases. *Z. Phys. Chemie* 85: 297-328.

[5] 1929. Molecular spectra and molecular structure; a general discussion. *Trans. Faraday Soc*. 25: 611-949.

[6] 1931. Photochemical processes; a general discussion. *Trans. Faraday. Soc*. 27: 357-573.

[7] Herzberg G, Scheibe G. 1929. On the absorption spectra of methyl halides and some other methyl compounds in the ultraviolet and in the Schumann region. *Trans. Faraday Soc*. 25: 716-717.

[8] Henri V. 1929. Absorption spectra of polyatomic molecules. Predissociation and dissociation of these molecules. *Trans. Faraday Soc*. 25: 765-767.

[9] Terenin A, Neujmin H. 1934. Photodissociation of molecules in the Schumann ultraviolet. *Nature* 134: 255.

[10] Mele A, Okabe H. 1969. Distribution of the excess energy in CN Produced in photodissociation of cyanogen halides and hydrogen cyanide. *J. Chem. Phys*. 51: 4798-4808.

[11] Basco N, Norrish, RGW. 1961. Vibrationally excited nitric oxide produced by the flash photolysis of nitrosyl chloride. *Nature* 189: 455-456.

[12] Basco N, Nicholas JE, Norrish RGW, Vickers WHJ. 1963. Vibrationally excited cyanogen radicals produced in the flash photolysis of cyanogen and cyanogen halides. *Proc. Roy. Soc. A* 272: 147-163.

[13] Welge KH, Stuhl F. 1967. Energy distribution in the photodissociation $H_2O \rightarrow H(1^2S)+OH(X^2\Pi)$. *J. Chem. Phys*. 46: 2440-2441.

[14] Riley SJ, Wilson KR. 1972. Excited fragments from excited molecules: Energy partitioning in the photodissociation of alkyl iodides. *Discuss. Faraday Soc*. 53: 132-146.

[15] Sparks RK, Carlson LR, Shobotake K, Kowalczyk ML, Lee YT. 1980. Ozone photolysis: A determination of the electronic and vibrational state distributions of primary products. *J. Chem. Phys*. 72: 1401-1402.

[16] Zare RN. 1972. Photoejection dynamics. *Mol. Photochem*. 4: 1-37.

[17] Dzvonik M, Yang S, Bersohn R. 1974. Photodissociation of molecular beams of aryl halides. *J. Chem. Phys*. 61: 4408-4421.

[18] Schultz A, Zare RN, Cruse HW. 1972. Laser-induced fluorescence – method to measure internal state distribution of reaction products. *J. Chem. Phys*. 57: 1354-1355.

[19] See, for example, Kinsey JL. 1977. Laser-induced fluorescence. *Annu. Rev. Phys. Chem*. 28: 349-372.

[20] See, for example, Ashfold MNR, Howe JD. 1994. Multiphoton Spectroscopy of Molecular Species. *Annu. Rev. Phys. Chem*. 45: 57-82.

[21] Greene CH, Zare RN. 1982. Photofragment alignment and orientation. *Annu. Rev. Phys. Chem*. 33: 119-150.

[22] Dixon RN. 1986. The determination of the vector correlation between photofragment rotational and translational motions from the analysis of Doppler broadened spectral-line profiles. *J. Chem. Phys.* 85: 1866-1879.

[23] Hall GE, Houston PL 1989. Vector correlations in photodissociation dynamics. *Annu. Rev. Phys. Chem.* 40: 375-405.

[24] Chandler DW, Houston PL. 1987. Two-dimensional imaging of state-selected photodissociation products detected by multiphoton ionization. *J. Chem. Phys.* 87: 1445-1447.

[25] Heck AJR, Chandler DW. 1995. Imaging techniques for the study of chemical reaction dynamics. *Annu. Rev. Phys. Chem.* 46: 335-372.

[26] Eppink ATJB, Parker DH. 1997. Velocity map imaging of ions and electrons using electrostatic lenses: Application in photoelectron and photofragment ion imaging of molecular oxygen. *Rev. Sci. Instrum*. 68: 3477-3484.

[27] Ashfold MNR, Nahler NH, Orr-Ewing AJ, Vieuxmaire OPJ, Toomes RL, *et al*. 2006. Imaging the dynamics of gas phase reactions. *Phys. Chem. Chem. Phys*. 8: 26-53.

[28] Gebhardt CR, Rakitzis TP, Samartzis PC, Ladopoulos V, Kitsopoulos TN. 2001. Slice imaging: A new approach to ion imaging and velocity mapping. *Rev. Sci. Instrum*. 72: 3848-3853.

[29] Townsend D, Minitti MP, Suits AG. 2003. Direct current slice imaging. *Rev. Sci. Instrum*. 74: 2530-2539.

[30] Schnieder L, Meier W, Welge KH, Ashfold MNR, Western CM. 1990. Photodissociation dynamics of H_2S at 121.6 nm and a determination of the potential-energy function of $SH(A^2\Sigma^+)$. *J. Chem. Phys*. 92: 7027-7037.

[31] Harich SA, Hwang DWH, Yang X, Lin JJ, Yang X, Dixon RN. 2000. Photodissociation of H_2O at 121.6 nm: A state-to-state dynamical picture. *J. Chem. Phys*. 113: 10073-10090.

[32] Ashfold MNR, King GA, Murdock D, Nix MGD, Oliver TAA, Sage AG. 2010. $\pi\sigma^*$ states in molecular photochemistry. *Phys. Chem. Chem. Phys*. 12: 1218-1238.

[33] Zewail AH. 2000. Femtochemistry: Atomic-scale dynamics of the chemical bond. *J. Phys. Chem. A* 104: 5660-5694.

[34] Roberts GM, Stavros VG. 2014. The role of $\pi\sigma^*$ states in the photochemistry of heteroaromatic biomolecules and their subunits: insights from gas-phase femtosecond spectroscopy. *Chem. Sci*. 5: 1698-1722.

[35] Stolow A, Bragg AE, Neumark DM. 2004. Femtosecond time-resolved photoelectron spectroscopy. *Chem. Rev*. 104: 1719-1757.

[36] Suzuki T. 2006. Femtosecond time-resolved photoelectron imaging. *Annu. Rev. Phys. Chem*. 57: 555-592.

[37] Worth GA, Cederbaum LS. 2004. Beyond Born-Oppenheimer: molecular dynamics through a conical intersection. *Annu. Rev. Phys. Chem.* 55: 127-158.

[38] Matsika S, Krause P. 2011. Non-adiabatic events and conical intersections. *Annu. Rev. Phys. Chem.* 62: 621-643.

[39] Domcke W, Yarkony DR. 2012. Role of conical intersections in molecular spectroscopy and photoinduced chemical dynamics. *Annu. Rev. Phys. Chem.* 63: 325-352.

[40] See, for example, Song Y, Lucas M, Alcaraz M, Zhang JS, Brazier C. 2105. Ultraviolet photodissociation dynamics of the allyl radical via the $B^2A_1(3s)$, $C^2B_2(3p_y)$, and $E^2B_1(3p_x)$ electronic excited states. *J. Phys. Chem. A* 119: 12318-12328.

[41] See, for example, Shapero M, Cole-Filipiak NC, Haibach-Morris C, Neumark DM. 2015. Benzyl radical photodissociation dynamics at 248 nm. *J. Phys. Chem. A* 119: 12349-12356.

[42] See, for example, De Vries MS, Hobza P. 2007. Gas phase spectroscopy of biomolecular building blocks. *Annu. Rev. Phys. Chem*. 58: 585-612.

[43] Van de Meeraker SYT, Bethlem HL, Vanhaecke N, Meijer G. 2012. Manipulation and control of molecular beams. *Chem. Rev.* 112: 4828-4878.

[44] Krausz F, Ivanov M. 2009. Attosecond physics. *Rev. Mod. Phys*. 81: 163-234.

[45] Sansone G., Kelkensberg F, Perez-Torres JF, Morales F, Kling MF, *et al*. 2010. Electron localisation following attosecond molecular photoionisation. *Nature* 465: 763-766.

[46] Hoener M, Fang L, Komilov O, Gessner O, Pratt ST, *et al*. 2010. Ultraintense X-ray induced ionization, dissociation, and frustrated absorption in molecular nitrogen. *Phys. Rev. Lett*. 104: 253002.

[47] Kupper J, Stern S, Holmegaard L, Filsinger F, Rouzee A. 2014. X-ray diffraction from isolated and strongly aligned gas-phase molecules with a free-electron laser. *Phys. Rev. Lett.* 112: 083002.

[48] Franck J, Rabinowitsch E. 1934. Some remarks about free radicals and the photochemistry of solutions. *Trans. Faraday Soc*. 30: 120-130.

[49] Meadows, LF, Noyes RM. 1960. The dependence on wavelength of quantum yields for iodine dissociation. *J. Amer. Chem. Soc*. 82: 1872-1876.

[50] Porter G. 1968. Flash photolysis and some of its applications. *Science* 160: 1299-1307.

[51] Porter G, Topp MR. 1968. Nanosecond flash photolysis and the absorption spectra of excited singlet states. *Nature*. 220: 1228-1229.

[52] Chuang TJ, Hoffman GW, Eisenthal KB. 1974. Picosecond studies of cage effect and collision-induced predissociation of iodine in liquids. *Chem. Phys. Lett.* 25: 201-205.

[53] Harris AL, Brown JK, Harris CB. 1988. The nature of simple photodissociation reactions in liquids on ultrafast time scales. *Annu. Rev. Phys. Chem*. 39: 341-366.

[54] Kliner DAV, Alfano JC, Barbara PF. 1993. Photodissociation and vibrational relaxation of I_2^- in ethanol. *J. Chem. Phys.* 98: 5375-5389.

[55] Scherer NF, Ziegler LD, Fleming GR. 1992. Heterodyne-detected time-domain measurement of I_2 predissociation and vibrational dynamics in solution. *J. Chem. Phys.* 96: 5544–5547

[56] Banin U, Ruhman S. 1993. Ultrafast photodissociation of I_3. Coherent photochemistry in solution. *J. Chem. Phys.* 98: 4391-4403.

[57] Reid PJ. 2001. Understanding the Phase-Dependent Reactivity of Chlorine Dioxide Using Resonance Raman Spectroscopy. *Acc. Chem. Res.* 34: 691-698.

[58] Owrutsky JC, Raftery D, Hochstrasser RM. 1994. Vibrational relaxation dynamics in solutions. *Annu. Rev. Phys. Chem.* 45: 519-555.

[59] Horng ML, Gardecki JA, Papazyan A, Maroncelli M. 1995. Subpicosecond measurements of polar solvation dynamics: coumarin 153 revisited. *J. Phys. Chem.* 99: 17311-17337.

[60] Stratt RM, Maroncelli M. 1996. Non-reactive dynamics in solution: the emerging molecular view of solvation dynamics and vibrational relaxation. *J. Phys. Chem.* 100: 12981-12996.

[61] Philpott MJ, Hayes SC, Reid PJ. 1998. Femtosecond pump–probe studies of chlorine dioxide photochemistry in water and acetonitrile. *Chem. Phys.* 236: 207-224.

[62] Zhang JZ, Harris CB. 1991. Photodissociation dynamics of $Mn_2(CO)_{10}$ in solution on ultrafast time scales. *J. Chem. Phys.* 95: 4024-4032.

[63] Moore JN, Hansen PA, Hochstrasser RM. 1989. Picosecond infrared probing of metal-carbonyl photodissociation products. *J. Amer. Chem. Soc.* 111: 4563-4566.

[64] Anfinrud PA, Han C, Hochstrasser RM. 1989. Direct observations of ligand dynamics in hemoglobin by subpicosecond infrared spectroscopy. *Proc. Natl. Acad. Sci. U.S.A.* 86: 8387-8391.

[65] Wilhelm T, Piel J, Riedle E. 1997. Sub-20-fs pulses tunable across the visible from a blue-pumped single-pass noncollinear parametric converter. *Opt. Lett.* 22: 1494-1496.

[66] Berera R, van Grondelle R, Kennis JTM. 2009. Ultrafast transient absorption spectroscopy: principles and application to photosynthetic systems. *Photosyn. Res.* 101: 105-118.

[67] Thomsen CL, Madsen D, Keiding SR, Thøgersen J, Christiansen O. 1999. Two-photon dissociation and ionization of liquid water studied by femtosecond transient absorption spectroscopy. *J. Chem. Phys.* 110: 3453-3462.

[68] Moskun AC, Jailaubekov AE, Bradforth SE. 2006. Rotational coherence and a sudden breakdown in linear response seen in room-temperature liquids. *Science*. 311: 1907-1911.

[69] Hamm P, Lim M, Hochstrasser RM. 1998. Structure of the amide I band of peptides measured by femtosecond nonlinear-infrared spectroscopy. *J. Phys. Chem. B*. 102: 6123-6138.

[70] Hybl JD, Albrecht Ferro A, Jonas DM. 2001. Two-dimensional Fourier transform electronic spectroscopy. *J. Chem. Phys.* 115: 6606-6622.

[71] Ruetzel S, Diekmann M, Nuernberger P, Walter C, Engels B, Brixner T. 2014. Multidimensional spectroscopy of photoreactivity. *Proc. Natl. Acad. Sci. U.S.A.* 111: 4764-4769.

[72] Elles CG, Crim FF. 2006. Connecting chemical dynamics in gas and liquids. *Annu. Rev. Phys. Chem.* 57: 273-302.

[73] Harris SJ, Murdock D, Zhang Y, Oliver TAA, Grubb MP, *et al*., 2013. Comparing molecular photofragmentation dynamics in the gas and liquid phases. *Phys. Chem. Chem. Phys.* 15: 6567-6582.

[74] Sobolewski AL, Domcke W, Dedonder-Lardeux C, Jouvet C. 2002. Excited-state hydrogen detachment and hydrogen transfer by repulsive $^1\pi\sigma^*$ states: A new paradigm for nonradiative decay in aromatic biomolecules. *Phys. Chem. Chem. Phys.* 4: 1093-1100.

[75] Ashfold MNR, Cronin B, Devine AL, Dixon RN, Nix MGD. 2006. The role of $\pi\sigma^*$ states in the near ultraviolet photodissociation of heteroaromatic molecules. *Science* 312: 1637-1640.

[76] Oliver TAA, King GA, Tew DP, Dixon RN, Ashfold MNR. 2012. Controlling the electronic product branching at conical intersections in the UV photolysis of *para*-substituted thiophenols. *J. Phys. Chem. A* 116: 12444-12459.

[77] Devine AL, Nix MGD, Dixon RN, Ashfold MNR. 2008. Near ultraviolet photodissociation of thiophenol. *J. Phys. Chem. A* 112: 9563-9574.

[78] Nix MGD, Devine AL, Cronin B, Dixon RN, Ashfold MNR. 2006. High resolution photofragment translational spectroscopy studies of the near ultraviolet photolysis of phenol. *J. Chem. Phys.* 125:133318.

[79] Dixon RN, Oliver TAA, Ashfold MNR. 2011. Tunnelling under a conical intersection: Application to the product vibrational state population distributions in the UV photodissociation of phenols. *J. Chem. Phys.* 134:194303.

[80] Karsili TNV, Wenge AM, Murdock D, Harris SJ, Harvey JN, *et al*. 2013. O–H bond fission in 4-substituted phenols: S_1 state predissociation viewed in a Hammett-like framework. *Chem. Sci*. 4: 2434-2446.

[81] Sobolewski AL, Domcke W. 2001. Photoinduced electron and proton transfer in phenol and its clusters with water and ammonia. *J. Phys. Chem. A* 105: 9275-9283.

[82] Ramesh SG, Domcke W. 2013. A multi-sheeted three-dimensional potential-energy surface for the H-atom photodissociation of phenol. *Farad. Discuss.* 163: 73-94.

[83] Yang KR, Xu X, Zheng JJ, Truhlar DG. 2014. Full-dimensional potentials and state couplings and multidimensional tunnelling calculations for the photodissociation of phenol. *Chem. Sci*. 5: 4661-4680.

[84] Zhu X, Malbon CL, Yarkony DR. 2016. An improved quasi-diabatic representation of the 1, 2, 3^1A coupled adiabatic potential energy surfaces of phenol in the full 33 internal coordinates. *J. Chem. Phys*. 144: 124312.

[85] Venkatesan TS, Ramesh SG, Lan Z, Domcke W. 2012. Theoretical analysis of photoinduced H-atom elimination in thiophenol. *J. Chem. Phys*. 136: 174312.

[86] Roberts GM, Chatterly AS, Young JD, Stavros VG. 2012. Direct observation of hydrogen tunnelling dynamics in photoexcited phenol. *J. Phys. Chem. Lett*. 3: 348-352.

[87] Wenge AM, Karsili TNV, Rodriguez JD, Cotterell MI, Marchetti B, *et al*. 2015. Tuning photochemistry: substituent effects on $\pi\sigma^*$ state mediated bond fission in thioanisoles. *Phys. Chem. Chem. Phys*. 17: 16246-16256.

[88] Lim JS, Kim SK. 2010. Experimental probing of conical intersection dynamics in the photodissociation of thioanisole. *Nat. Chem*. 2: 627-632.

[89] Roberts GM, Hadden DJ, Bergendahl LT, Wenge AM, Harris SJ, *et al*. 2013. Exploring quantum phenomena and vibrational control in σ^* mediated photochemistry. *Chem. Sci.* 4: 993-1001.

[90] Hoshino-Nagasaka M, Suzuki T, Ichimura T, Kasahara S, Baba M, *et al*. 2010. Rotationally resolved high-resolution spectrum of the S_1–S_0 transition of jet-cooled thioanisole. *Phys. Chem. Chem. Phys*. 12: 13243-13247.

[91] Han SH, Lim JS, Yoon JH, Lee JM, Kim SY, *et al*. 2014. Conical intersection seam and bound resonances embedded in continuum observed in the photodissociation of thioanisole-d_3. *J. Chem. Phys*. 140: 054307.

[92] You HS, Han S, Yoon JH, Lim JS, Lee J. *et al*. 2015. Structure and dynamic role of conical intersections in the $\pi\sigma^*$-mediated photodissociation reactions. *Int. Rev. Phys. Chem*. 34: 429-459.

[93] Xie CJ, Ma JY, Zhu XL, Yarkony DR, Xie DQ, Guo H. 2016. Nonadiabatic tunneling in photodissociation of phenol. *J. Amer. Chem. Soc.*, 138: 7828-7831, and references therein.

[94] Li SHL, Xu XF, Hoyer CE, Truhlar DG. 2015. Non-intuitive diabatic potential energy surfaces for thioanisole. *J. Phys. Chem. Lett*. 6: 3352-3359.

[95] Li SHL, Xu XF, Truhlar DG. 2015. Computational simulation and interpretation of the low-lying electronic states and electronic spectrum of thioanisole. *Phys. Chem. Chem. Phys*. 17: 20093-20099.

[96] Hermann R, Dey GR, Naumov S, Brede O. 2000. Thiol radical cations and thiyl radicals as direct products of the free electron transfer from aromatic thiols to n-butyl chloride radical cations. *Phys. Chem. Chem. Phys*. 2: 1213-1220.

[97] Riyad YM, Naumov S, Hermann R, Brede O. 2006. Deactivation of the first excited singlet state of thiophenols. *Phys. Chem. Chem. Phys*. 8: 1697-1706.

[98] Zhang Y, Oliver TAA, Das S, Roy A, Ashfold MNR, Bradforth SE. 2013. Exploring the energy disposal immediately after bond-breaking in solution: the wavelength-dependent excited state dissociation pathways of para-methylthiophenol. *J. Phys. Chem. A* 117: 12125-12137.

[99] Zhang Y, Oliver TAA, Ashfold MNR, Bradforth SE. 2012. Contrasting the excited state reaction pathways of phenol and para-methylthiophenol in the gas and liquid phases. *Farad. Discuss*. 157: 141-163.

[100] Murdock D, Harris SJ, Karsili TNV, Greetham GM, Clark IP, *et al*. 2012. Photofragmentation dynamics in solution probed by transient IR absorption spectroscsopy:πσ*-mediated bond cleavage in *p*-methylthiophenol and *p*-methylthioanisole. *J. Phys. Chem. Letts*. 3: 3715-3720.

[101] Porter G; Wright FJ. 1955. Primary photochemical processes in aromatic molecules. Part 3. Absorption spectra of benzyl, anilino, phenoxy and related free radicals. *Trans. Faraday Soc*. 51: 1469−1474.

[102] Chen XY, Larsen DS, Bradforth SE, van Stokkum IHM. 2011. Broadband spectral probing revealing ultrafast photochemical branching after ultraviolet excitation of the aqueous phenolate anion. *J. Phys. Chem. A* 115: 3807-3819.

[103] Creed D. 1984. The photophysics and photochemistry of the near-UV absorbing amino acids-II. Tyrosine and its simple derivatives. *Photochem. Photobiol*. 39: 563−575.

[104] Oliver TAA, Zhang Y, Roy A, Ashfold MNR, Bradforth SE. 2015. Exploring autoionization and photoinduced proton-coupled electron transfer pathways of phenol in aqueous solution. *J. Phys. Chem. Lett*. 6: 4159-4164.

[105] Chen XY, Bradforth SE. 2008. The ultrafast dynamics of photodetachment. *Annu. Rev. Phys. Chem*. 59: 203-231.

[106] Westlake BC, Brennaman MK, Concepcion JJ, Paul JJ, Bettis SE, *et al*. 2011. Concerted electron-proton transfer in the optical excitation of hydrogen-bonded dyes. *Proc. Nat. Acad. Sci. U.S.A*. 108: 8554-8558.

[107] Goyal P, Schwerdtfeger CA, Soudackov AV, Hammes-Schiffer S. 2016. Proton quantization and vibrational relaxation in nonadiabatic dynamics of photoinduced proton-coupled electron transfer in a solvated phenol-amine complex. *J. Phys. Chem. B* 120: 2407-2417.

[108] Grubb MP, Coulter PM, Marroux HJB, Hornung B, McMullen RS, *et al*. 2016. Translational, rotational and vibrational relaxation dynamics of a solute molecule in a non-interacting solvent. *Nature Chem.* DOI: 10.1038/NCHEM.2570.

[109] Roberts GM, Marroux HJB, Grubb MP, Ashfold MNR and Orr-Ewing AJ. 2014. On the participation of photo-induced N–H bond fission in aqueous adenine at 266 and 220 nm: a combined ultrafast transient electronic and vibrational absorption spectroscopy study. *J. Phys. Chem. A* 118: 11211-11225.

[110] Blank DA, North SW, Lee YT. 1994. The ultraviolet photodissociation dynamics of pyrrole. *Chem. Phys.* 187: 35-47.

[111] Salzmann S, Kleinschmidt M, Tatchen J, Weinkauf R, Marian CM. 2008. Excited states of thiophene: ring opening as deactivation mechanism. *Phys. Chem. Chem. Phys.* 10: 380-392.

[112] Weinkauf R, Lehr L, Schlag EW, Salzmann S, Marian CM. 2008. Ultrafast dynamics in thiophene by femtosecond pump probe photoelectron spectroscopy and theory. *Phys. Chem. Chem. Phys*. 10: 393-404.

[113] Wu XF, Zheng XM, Wang HG, Zhao YY, Guan XG, *et al*. 2010. A resonance Raman spectroscopic and CASSCF investigation of the Franck-Condon region structural dynamics and conical intersections of thiophene. *J. Chem. Phys*. 133: 134507.

[114] Cui GL, Fang WH. 2011. Ab initio trajectory surface-hopping study on ultrafast deactivation process of thiophene. *J. Phys. Chem. A* 115: 11544–11550.

[115] Stenrup M. 2012. Theoretical study of the radiationless deactivation mechanisms of photo-excited thiophene. *Chem. Phys*. 397: 18-25.

[116] Prlj A, Curchod BFE, Corminboeuf C. 2015. Excited state dynamics of thiophene and bithiophene: new insights into theoretically challenging systems. *Phys. Chem. Chem. Phys*. 17: 14719-14730.

[117] Gavrilov N, Salzmann S, Marian CM. 2008. Deactivation by ring opening: a quantum chemical study of the excited states of furan and comparison to thiophene. *Chem. Phys*. 349: 269-277.

[118] Grimov EV, Léveque C, Gatti F, Burghardt I, Köppel H. 2011. Ab initio quantum study of photoinduced ring opening in furan. *J. Chem. Phys*. 135: 164305.

[119] Stenrup M, Larson Å. 2011. A computational study of radiationless deactivation mechanisms of furan. *Chem. Phys*. 379: 6-12.

[120] Vazdar M, Eckert-Maksic M, Barbatti M, Lischka H. 2009. Excited-state non-adiabatic dynamics simulations of pyrrole. *Mol. Phys*. 107: 845-854.

[121] Barbatti M, Lischka H, Salzmann S, Marian CM. 2009. UV excitation and radiationless deactivation of imidazole. *J. Chem. Phys*. 130: 034305.

[122] Szabla R, Tuna D, Góra RW, Šponer J, Sobolewski AL, Domcke W. 2013. Photochemistry of 2-aminooxazole, a hypothetical prebiotic precursor of RNA nucleotides. *J. Phys. Chem. Lett*. 4: 2785-2788.

[123] Perun S, Sobolewski AL, Domcke W. 2005. Photostability of 9*H*-adenine: mechanisms of the radiationless deactivation of the lowest excited singlet states. *Chem. Phys*. 313: 107-112.

[124] Liu FY, Morokuma K. 2013. Multiple pathways for the primary step of the spyropyran photochromic reaction: a CASPT2/CASSCF study. *J. Amer. Chem. Soc*. 135: 10693-10702.

[125] Prager S, Burghardt I, Dreuw A. 2014. Ultrafast C_{spiro}–O dissociation via a conical intersection drives spyropyran to merocyanine photoswitching. *J. Phys. Chem. A* 118: 1339-1349.

[126] Tuna D, Sobolewski AL, Domcke W. 2014. Electronically excited states and photochemical reaction mechanisms of β-glucose. *Phys. Chem. Chem. Phys*. 16: 38-47.

[127] Breda S, Reva I, Fausto R. 2009. UV-induced unimolecular photochemistry of 2(5H)-furanone and 2(5H)-thiophenone isolated in low temperature inert matrices. *Vib. Spectrosc*. 50: 57-67.

[128] Murdock D, Harris SJ, Luke J, Grubb MP, Orr-Ewing AJ, *et al*. 2014. Transient UV-pump-IR probe investigation of heterocyclic ring-opening dynamics in the solution phase: the role played by nσ* states in the photoinduced reactions of thiophenone and furanone. *Phys. Chem. Chem. Phys*. 16: 21271-21279.

[129] Murdock D, Ingle RA, Sazanovich IV, Clark IP, Harabuchi Y, *et al*., 2016. Contrasting ring-opening propensities in UV-excited α-pyrone and coumarin. *Phys. Chem. Chem. Phys*. 18: 2629-2638.

[130] Arnold BR, Brown CE, Lusztyk J. 1993. Solution photochemistry of 2*H*-pyran-2-one: laser flash photolysis with infrared detection of transients. *J. Amer. Chem. Soc*. 115: 1576-1577.

[131] Murdock D, Clark IP, Ashfold MNR. 2016. Probing photochemically and thermally-driven isomerisation reactions in α-pyrone. *J. Phys. Chem. A* (submitted).

[132] Maeda S, Harabuchi Y, Taketsuga T, Morokuma K. 2014. Systematic exploration of the minimum energy conical intersection structures near the Franck-Condon region. *J. Phys. Chem. A* 118: 12050-12058.

[133] Krauter CM, Moehring J, Buckup T, Pempointer M, Motzkus M. 2013. Ultrafast branching in the excited state of coumarin and umbelliferone. *Phys. Chem. Chem. Phys*. 15: 17846-17861.

[134] Zhang F, Cao ZZ, Qin X, Liu YZ, Wang YM, et al. 2008. C–Br bond dissociation mechanisms of 2-bromothiophene and 3-bromothiophene at 267 nm. *Acta Phys.-Chim. Sin.* 24: 1335-1341.

[135] Marchetti B, Karsili TNV, Kelly O, Kapetanopoulos P, Ashfold MNR. 2015. Near ultraviolet photochemistry of 2-bromo- and 2-iodothiophene: Revealing photoinduced ring opening in the gas phase? *J. Chem. Phys*. 142: 224303.

[136] Gougousi T, Samartzis PC, Kitsopoulos TN. 1998. Photodissociation study of CH_3Br in the first continuum. *J. Chem. Phys*. 108: 5742-5746.

[137] Ingle RA, Karsili TNV, Dennis GJ, Staniforth M, Stavros VG, *et al*. 2016. Extreme population inversion in the fragments formed by UV photoinduced S–H bond fission in 2-thiophenethiol. *Phys. Chem. Chem. Phys*. 18: 11401-11410.